Development/Plasticity/Repair

A Proinflammatory Stimulus Disrupts Hippocampal Plasticity and Learning via Microglial Activation and 25-Hydroxycholesterol

Yukitoshi Izumi,[3] Anil G. Cashikar,[1,3] Kathiresan Krishnan,[2] Steven M. Paul,[1,3] Douglas F. Covey,[1,2,3] Steven J. Mennerick,[1,3] and Charles F. Zorumski[1,3]

[1]Department of Psychiatry, Washington University School of Medicine in St. Louis, St. Louis, Missouri 63110-1010, [2]Department of Developmental Biology, Washington University School of Medicine in St. Louis, St. Louis, Missouri 63110, and [3]Taylor Family Institute for Innovative Psychiatric Research, Washington University School of Medicine in St. Louis, St. Louis, Missouri 63110-1093

Inflammatory cells, including macrophages and microglia, synthesize and release the oxysterol 25-hydroxycholesterol (25HC), which has antiviral and immunomodulatory properties. Here, we examined the effects of lipopolysaccharide (LPS), an activator of innate immunity, on 25HC production in microglia, and the effects of LPS and 25HC on CA1 hippocampal synaptic plasticity and learning. In primary microglia, LPS markedly increases the expression of cholesterol 25-hydroxylase (Ch25h), the key enzyme involved in 25HC synthesis, and increases the levels of secreted 25HC. Wild-type microglia produced higher levels of 25HC than *Ch25h* knock-out (KO) microglia with or without LPS. LPS treatment also disrupts long-term potentiation (LTP) in hippocampal slices via induction of a form of NMDA receptor-dependent metaplasticity. The inhibitory effects of LPS on LTP were mimicked by exogenous 25HC, and were not observed in slices from *Ch25h* KO mice. *In vivo*, LPS treatment also disrupts LTP and inhibits one-trial learning in wild-type mice, but not *Ch25h* KO mice. These results demonstrate that the oxysterol 25HC is a key modulator of synaptic plasticity and memory under proinflammatory stimuli.

Key words: **lipopolysaccharide; long-term potentiation; memory; metaplasticity; neurosteroids; oxysterols**

Significance Statement

Neuroinflammation is thought to contribute to cognitive impairment in multiple neuropsychiatric illnesses. In this study, we found that a proinflammatory stimulus, LPS, disrupts hippocampal LTP via a metaplastic mechanism. The effects of LPS on LTP are mimicked by the oxysterol 25-hydroxycholesterol (25HC), an immune mediator synthesized in brain microglia. Effects of LPS on both synaptic plasticity and one-trial inhibitory avoidance learning are eliminated in mice deficient in Ch25h (cholesterol 25-hydroxylase), the primary enzyme responsible for endogenous 25HC synthesis. Thus, these results indicate that 25HC is a key mediator of the effects of an inflammatory stimulus on hippocampal function and open new potential avenues to overcome the effects of neuroinflammation on brain function.

Introduction

Neuroinflammation and microglial activation appear to contribute to the pathophysiology of multiple neuropsychiatric disorders including neurodegenerative illnesses such as Alzheimer's disease (Wang and Colonna, 2019) and possibly even psychiatric disorders, including schizophrenia and major depression (Lathe et al., 2014; Hodes et al., 2015; Yirmiya et al., 2015; Iwata et al., 2016). All of these disorders are associated with significant cognitive impairment that contributes to disability and illness burden (Wohleb et al., 2016). Mechanisms underlying inflammation-associated cognitive impairment include microglia-secreted factors that contribute to synaptic dysfunction and impaired synaptic plasticity necessary for learning and memory (Wu et al., 2015).

In peripheral macrophages, the cholesterol-derived oxysterol 25-hydroxycholesterol (25HC), the predominant oxysterol produced

Received July 22, 2021; revised Oct. 12, 2021; accepted Oct. 17, 2021.

Author contributions: Y.I., A.G.C., and C.F.Z. designed research; Y.I. and A.G.C. performed research; K.K. and D.F.C. contributed unpublished reagents/analytic tools; Y.I., A.G.C., and C.F.Z. analyzed data; Y.I., A.G.C., K.K., S.M.P., D.F.C., S.J.M., and C.F.Z. wrote the paper.

This work was supported by National Institutes of Health | National Institute of Mental Health Grants MH-101874 (to S.J.M. and C.F.Z.), MH-114866 (to C.F.Z.), MH-123748 (S.J.M.), and MH-122379 (to. C.F.Z. and S.J.M.); the Taylor Family Institute for Innovative Psychiatric Research; and the Bantly Foundation. We thank Ann Benz and Kazuko Izumi for technical assistance, and members of the Taylor Family Institute for comments and advice.

S.M.P. and C.F.Z. serve on the Scientific Advisory Board of Sage Therapeutics. S.M.P. and D.F.C. were cofounders of Sage Therapeutics. D.F.C., S.M.P., and C.F.Z. have equity in Sage Therapeutics. Sage Therapeutics did not fund this research. S.M.P. is employed by Karuna Therapeutics. The authors declare no other competing financial interests.

Correspondence should be addressed to Charles F. Zorumski at zorumskc@wustl.edu.

https://doi.org/10.1523/JNEUROSCI.1502-21.2021

and released from macrophages (Blanc et al., 2013), contributes to inflammatory responses. Proinflammatory stimuli, including the bacterial cell wall endotoxin lipopolysaccharide (LPS) and other monocyte activators (Bauman et al., 2009; Gold et al., 2014; Luu et al., 2016), promote the expression of cholesterol-25-hydroxylase (Ch25h), the principal enzyme responsible for 25HC synthesis (Lund et al., 1998). Similar changes in Ch25h and 25HC following inflammatory stimuli are seen in brain, raising the possibility that 25HC is an important mediator of neuroinflammation, potentially impacting neural circuits and behavior (Min et al., 2009; Waltl et al., 2013; Simon, 2014; Jang et al., 2016).

We have previously reported that 24S-HC, a side chain oxidized derivative of cholesterol synthesized by CYP46A1 in neurons, is a potent positive allosteric modulator (PAM) of NMDARs, a class of glutamate receptors that triggers learning-related synaptic plasticity (Paul et al., 2013; Sun et al., 2016a,b). Additionally, we found that 25HC is a partial oxysterol agonist with weaker PAM activity at NMDARs and is a functional inhibitor of the effects of 24S-HC on NMDARs (Linsenbardt et al., 2014). In the present study, we examined the effects of a known proinflammatory stimulus, LPS, on the production of 25HC in microglia and the effects of LPS and 25HC on long-term potentiation (LTP) in the CA1 region of the rodent hippocampus. We provide evidence that LPS stimulates enhanced expression of Ch25h and increases 25HC synthesis in microglia, and that both LPS and 25HC impair synaptic plasticity in the CA1 hippocampal region. The effects of LPS on hippocampal synaptic plasticity and on a one-trial learning task *in vivo* were not observed in Ch25h knock-out (KO) mice, suggesting that 25HC mediates or contributes to neuroinflammation-impaired learning and memory.

Materials and Methods

Animals. Homozygous Ch25h KO mice (*Ch25h* KO) backcrossed to C57BL/6J mice for >10 generations (Bauman et al., 2009) were obtained from The Jackson Laboratory (stock #016263). C57BL/6J mice (The Jackson Laboratory) were used as wild-type controls. Sprague Dawley albino rats were obtained from Harlan Laboratories and were housed in approved facilities at Washington University in St. Louis. Animal use followed National Institutes of Health guidelines and was approved by the Washington University in St. Louis Institutional Animal Care and Use Committee.

Microglia cultures. Primary mouse microglia were prepared from postnatal day 2 (P2) to P3 pups of both sexes from wild-type and *Ch25h* KO mice on a C57BL/6J background (Bohlen et al., 2017). Brains were dissected into HBSS (catalog #14175–079, Thermo Fisher Scientific). After removing the olfactory bulb, cerebellum, brainstem, and meninges, the cortices were transferred to 1 ml of warm TrypLE Express reagent (catalog #12605–010, Thermo Fisher Scientific) and incubated at 37°C for 10–20 min for tissue dissociation. Trypsin activity was stopped by addition of media containing 10% fetal bovine serum, triturated, filtered through a 100 µm nylon filter and plated in poly-D-lysine-coated T75 flasks in 20 ml culture media [DMEM/F12 containing 10% fetal bovine serum, GlutaMAX, Na-pyruvate, penicillin/streptomycin, and 5 ng/ml granulocyte-macrophage colony-stimulating factor (GM-CSF); catalog #1320–03-5, GOLDBIO]. After cells were confluent, the flasks were shaken at 200 rpm at 37°C for 30 min. Floating cells were collected, washed, counted, and plated in culture media without GM-CSF at a density of 10^6 cells/1000 mm^2. Because serum can decrease microglial activation and skew results, we used serum-free media modified from the study by Bohlen et al. (2017) containing DMEM/F12, 0.1% BSA, GlutaMAX, penicillin/streptomycin, *N*-acetyl cysteine and 1× ITS Media Supplement (catalog #AR013, R&D Systems).

Quantitative PCR. For gene expression studies, microglia were treated with 100 ng/ml LPS or PBS for 24 h in triplicate. RNA from treated microglia was isolated using Qiagen RNeasy Mini Kit. For cDNA synthesis, a first strand cDNA synthesis kit (igScript; Intact Genomics) was used. Relative gene expression was measured by quantitative PCR (qPCR) using PrimeTime Gene Expression Master Mix and Primetime probe-based assays for mouse *Ch25h* and *Actb* (actin) from Integrated DNA Technologies. Reactions were performed on StepOnePlus Real-Time PCR System (Thermo Fisher Scientific). Data analysis was performed using Expression Suite software (Thermo Fisher Scientific).

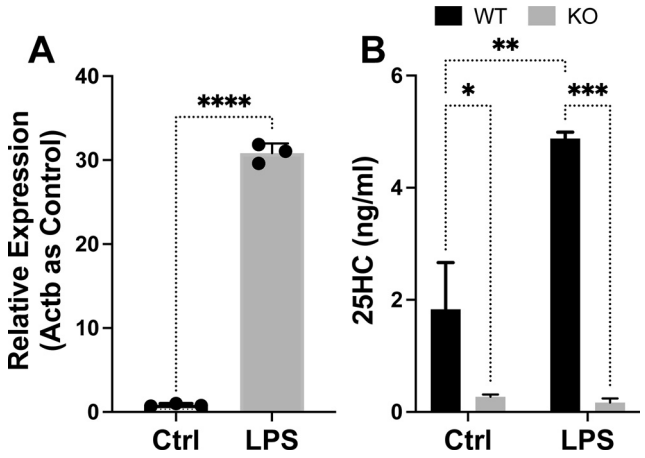

Figure 1. Expression of *Ch25h* and production of 25HC by microglia in response to LPS treatment for 24 h. ***A***, Ch25h gene expression was measured by qPCR and normalized to actin (Actb). Control and LPS values were compared by *t* tests. ***B***, Conditioned culture media from PBS vehicle control (Ctrl), LPS-treated wild-type (WT), or *Ch25h* KO microglia were used to estimate the amount of 25HC by liquid chromatography-mass spectrometry. Statistical significance was assessed using two-way ANOVA (adjusted *p* value: $*p < 0.05$, $**p < 0.005$, $***p < 0.0005$, $****p < 0.0001$).

Oxysterol measurements. Microglia cultures harvested by shaking mixed glial cultures, as described above, were plated in culture media without GM-CSF on uncoated plastic. On day 3, cells were washed with warm PBS and media was replaced with serum-free media with or without 100 ng/ml LPS. Following incubation for 24 h, media was harvested and centrifuged at 10,000 × *g* for 5 min at room temperature to remove cell debris. Supernatants were collected in fresh tubes and subjected to derivatization followed by liquid chromatography-mass spectrometry as described in the study by Jiang et al. (2007). The amount of 25HC was estimated based on the peak area of an internal standard of deutrated-25-hydroxycholesterol.

Hippocampal slice preparation. Hippocampal slices were prepared from P28 to P32 male albino rats or mice using previously described methods (Tokuda et al., 2010, 2011). Dissected hippocampi were pinned at their ventral pole on a 3.3% agar base in ice-cold artificial CSF (ACSF) containing the following (in mM): 124 NaCl, 5 KCl, 2 $MgSO_4$, 2 $CaCl_2$, 1.25 NaH_2PO_4, 22 $NaHCO_3$, and 10 glucose, bubbled with 95% O_2-5% CO_2 at 4–6°C. The dorsal two-thirds of the hippocampus was cut into 500 µm (rat) or 400 µm (mouse) slices using a rotary tissue slicer. Acutely prepared slices were kept in an incubation chamber containing gassed ACSF for at least 1 h at 30°C before further study.

Hippocampal slice physiology. For electrophysiological studies, slices were transferred to a submersion-recording chamber at 30°C with ACSF and perfused continuously at 2 ml/min. Extracellular recordings were obtained from the apical dendritic layer (stratum radiatum) of the CA1 region for monitoring EPSPs with electrodes filled with 2 M NaCl (5–10 MΩ resistance).

EPSPs were evoked using 0.1 ms constant current pulses through a bipolar stimulating electrode in the Schaffer collateral (SC) pathway. Baseline responses were monitored by applying single stimuli to the SC pathway every 60 s at half-maximal intensity based on a control input–output (IO) curve. After obtaining stable baseline recordings for at least 10 min, LTP was induced by a single 100 Hz × 1 s high-frequency stimulation (HFS) using the same intensity stimulus. Following HFS, responses were monitored by single stimuli

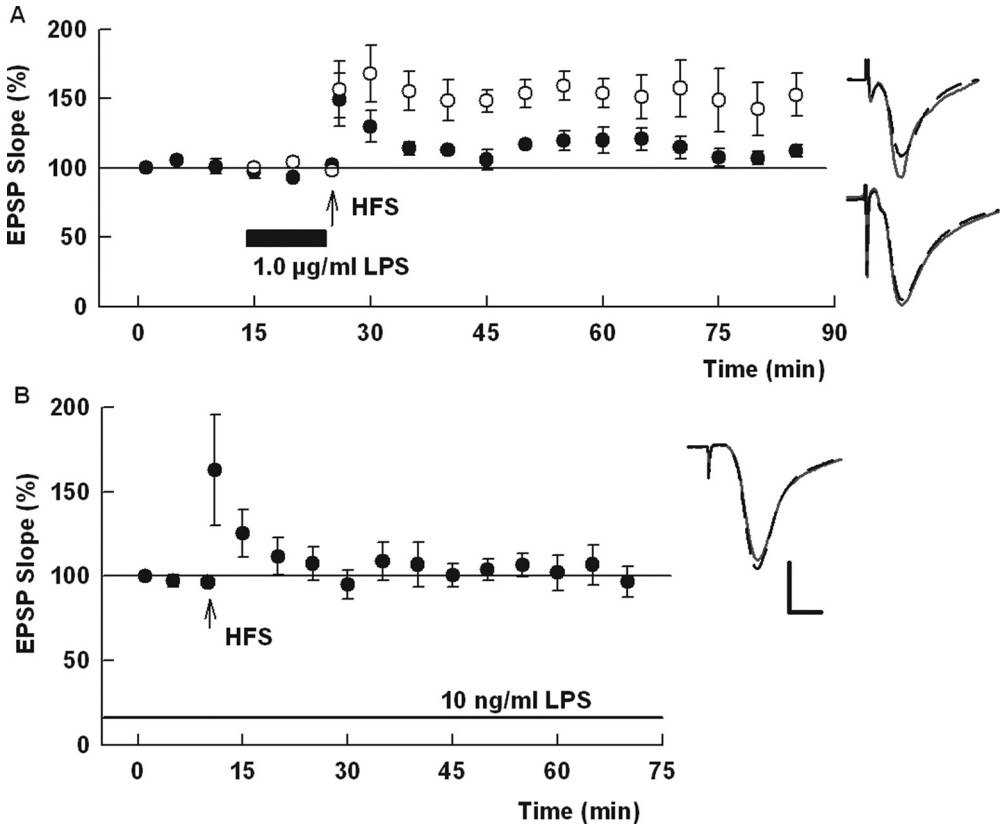

Figure 2. LPS inhibits LTP in the CA1 region of rat hippocampal slices. ***A***, When administered for 10 min just before 100 Hz × 1 s HFS, 1 µg/ml LPS (black bar) inhibited the induction of LTP induced by 100 Hz × 1 s HFS (arrow; black circles). Control LTP in naive hippocampal slices is shown in white circles. Traces to the right of this graph and in subsequent figures show representative EPSPs at baseline before HFS (dashed traces) and 60 min following HFS (red traces). ***B***, A low concentration of LPS (10 ng/ml) also inhibits LTP when administered for ≥1 h before and during slice recording. Calibration: 1 mV, 5 ms.

once per minute during the period of post-tetanic potentiation (PTP) and then every 5 min for the remainder of an experiment. For display purposes, graphs show data every 5 min except during initial PTP.

Isolated EPSPs mediated by NMDARs were recorded with very low-frequency SC stimulation (1/min) in ACSF containing 0.1 mM Mg^{2+} and 2.5 mM Ca^{2+}, to promote NMDAR activation, and 30 μM CNQX (6-cyano-7-nitroquinoxaline-2,3-dione), to eliminate the contribution of AMPARs to evoked EPSPs (Izumi et al., 2005).

Behavioral studies. Wild-type and *Ch25h* KO mice were tested for memory acquisition in a one-trial inhibitory avoidance learning task (Whitlock et al., 2006; Tokuda et al., 2010; Izumi and Zorumski, 2020; Izumi et al., 2021). The testing apparatus consists of two chambers, one of which is lit and the other is dark; both compartments have a floor of stainless steel rods (4 mm in diameter, spaced 10 mm apart) through which an electrical shock could be delivered in the dark chamber (12 × 20 × 16 cm). The adjoining safe (lit) compartment (30 × 20 × 16 cm) was illuminated with four 13 W lights. Light intensity in the lit chamber was 1000 lux, while that in the dark chamber was <10 lux. On the first day of testing, mice were placed in the lit chamber and allowed to habituate to the apparatus by freely moving between chambers for 10 min. No footshocks were given during this pre-exposure trial. On the next day, mice were administered LPS (1 mg/kg, i.p.) or vehicle (saline) 1 h before training. At the time of training, animals were initially placed in the lit compartment and allowed to explore the apparatus freely for up to 300 s (5 min). When the mice completely entered the dark chamber, they were immediately given a footshock. Upon returning to the lit (safe) chamber, animals were removed from the apparatus and returned to their home cages. On the next day of testing, mice were placed in the lit chamber without any drug treatment and the latency to enter the dark compartment was recorded over a 300 s trial.

Chemicals. Deuterated (d6) 25-hydroxycholesterol was purchased from Avanti Polar Lipids (catalog #700053). The enantiomer of 25HC was synthesized from Ent-Testosterone, as described previously (Westover and Covey, 2006; Linsenbardt et al., 2014). Minocycline and 25HC were from Sigma-Aldrich as was LPS, and phenol was extracted from *Escherichia coli* serotype O111:B4 (L2630). IAXO-102 was purchased from AdipoGen Life Sciences, and TAK-242 was purchased from R&D Systems. LPS from *Rhodobacter sphaeroides* (LPS-RS) was purchased from InvivoGen. Other chemicals and salts were obtained from Millipore Sigma. For microglial depletion experiments, wild-type mice were fed PLX5622 (Selleck Chemicals) formulated in chow (AIN-76A) at 1200 ppm (Research Diets) for 7–14 d, beginning at the time they were weaned, before preparing hippocampal slices. Drugs were prepared as stock solutions in either ACSF or DMSO and diluted to final concentration at the time of experiment.

Statistical analysis. Physiologic data were collected and analyzed using PClamp software (Molecular Devices). Data are expressed as the mean ± SEM 60 min following HFS and are normalized with respect to initial baseline recordings (taken as 100%). In most studies, a two-tailed Student's *t* test was used for comparisons between groups. In cases of non-normally distributed data, the nonparametric Wilcoxon rank-sum test was used. For experiments in wild-type and *Ch25h* KO mice, data were analyzed by two-way ANOVA followed by Tukey's multiple-comparison test. Statistical comparisons in physiological studies were based on IO curves at baseline and 60 min following HFS to determine the degree of change in EPSP slope at the 50% maximal point, with $p < 0.05$ considered to be significant. Statistical analyses were performed using commercial software (SigmaStat, Systat). Data shown in figures for physiological studies are derived from continuous monitoring of EPSPs at low frequency during the course of experiments and thus may differ from results described in the text, which represent analyses based on comparison of input–output curves before and 60 min following HFS.

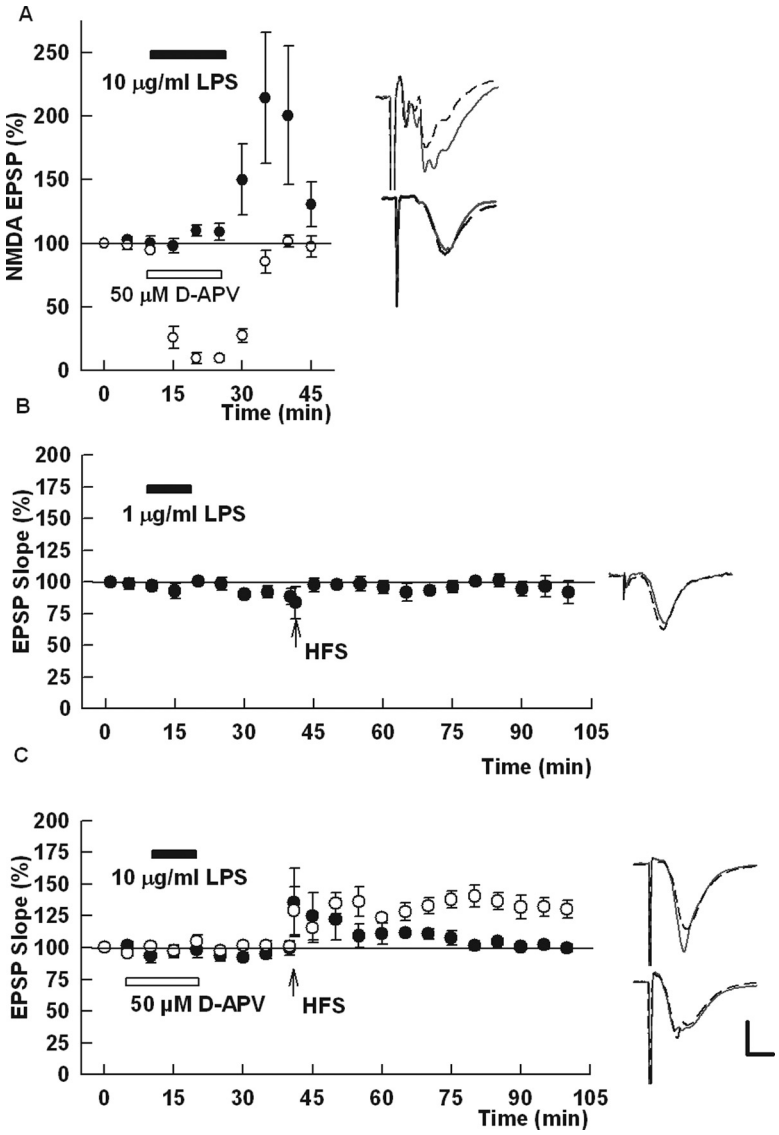

Figure 3. LPS produces a persistent LTP inhibition that is prevented by an NMDAR antagonist. ***A***, At 10 μg/ml, LPS produced a slowly developing increase in NMDAR-mediated EPSPs (black circles). This effect was completely inhibited by the NMDAR antagonist D-APV (white circles). Traces to the right of the graph show representative NMDAR EPSPs before (dashed traces) and 10 min following LPS administration (red traces). ***B***, LPS inhibited LTP when administered at 1 μg/ml for 10 min (black bar) and washed out 30 min before HFS (arrow). ***C***, Similar persisting LTP inhibition was observed with 10 μg/ml LPS (black bar, black circles). This prolonged LTP inhibition was completely reversed by coadministration of D-APV (white bar) during LPS perfusion (white circles); D-APV and LPS were washed out of the slices at the same time. Traces to the right of the graphs in ***B*** and ***C*** show representative EPSPs, as in Figure 1. Calibration: 1 mV, 5 ms.

Results

In initial experiments, we examined the effects of LPS on the expression of Ch25h and levels of 25HC in cultured microglia. At a concentration of 100 ng/ml, LPS treatment increased levels of Ch25h to ~30 times that of baseline after 24 h (Fig. 1*A*). As expected, microglia from *Ch25h*-deficient (*Ch25h* KO) mice had no expression of enzyme (data not shown). Consistent with enzyme expression data, levels of 25HC were increased by >200% in conditioned media of LPS-treated wild-type microglia compared with that of control (PBS)-treated microglia over the same period of time (Fig. 1*B*). On the other hand, conditioned media from *Ch25h*-deficient microglial cultures only showed very low levels of 25HC with no enhancement in the presence of LPS (Fig. 1*B*), indicating that Ch25h is the prime mediator of 25HC synthesis in these cells. We also note that wild-type microglia produced 6.8-fold higher levels of 25HC than did *Ch25h* KO microglia in the absence of LPS treatment (Fig. 1*B*; control samples: 1.83 ± 0.83 vs 0.27 ± 0.042 ng/ml, respectively).

To determine whether LPS alters hippocampal synaptic function, we examined effects in *ex vivo* hippocampal slices from rats and mice, focusing on studies in P28 to P32 albino rats in the majority of studies, except as otherwise noted. When administered for 10–30 min at concentrations of 1 and 10 μg/ml before and during a single 100 Hz × 1 s HFS, LPS disrupted LTP induction without significantly altering baseline synaptic responses [1 μg/ml: 102.4 ± 4.2% of baseline EPSP slope measured 60 min following HFS ($N = 5$) vs 137.4 ± 5.6% change in controls ($N = 5$; $p = 0.0011$; Fig. 2*A*); 10 μg/ml: 88.5 ± 5.8% of baseline 60 min following HFS ($N = 5$, $p = 0.0003$) vs control LTP]. A short (15–30 min) exposure to a lower concentration of LPS (100 ng/ml) failed to alter baseline synaptic responses or LTP [129.9 ± 8.0% of baseline ($N = 5$, $p = 0.4645$) vs control LTP]. However, longer preincubations with either 10 or 100 ng/ml LPS for 2–3 h resulted in a profound decrease in the ability of Schaffer collateral synapses to undergo LTP [10 ng/ml: 96.6 ± 5.9% of baseline EPSP slope measured 60 min following HFS ($N = 5$; $p = 0.0010$) vs control LTP (Fig. 2*B*); 100 ng/ml: 86.3 ± 9.7% of baseline EPSP slope ($N = 6$, $p = 0.0020$)].

The inhibition of LTP by LPS did not result from the block of NMDARs. At 10 μg/ml, LPS produced a slowly developing, but variable, enhancement rather than inhibition of NMDAR-mediated synaptic responses (214.2 ± 51.5% change; $N = 5$; Fig. 3*A*). The slowly developing augmentation of NMDAR responses was completely blocked by coadministration of the competitive NMDAR antagonist, D-2-amino-5-phosphonovalerate (D-APV; 101.7 ± 4.7%; $N = 5$; Fig. 3*A*). Variable enhancement but not inhibition of NMDAR responses by LPS was also observed at 100 ng/ml (145.2 ± 17.2% change 60 min following washout; $N = 5$).

The augmentation of NMDAR responses by LPS raises the possibility that LPS acts as an acute direct or indirect neuronal stressor to disrupt LTP induction. Previously, we have observed that several forms of neuronal stress result in untimely NMDAR activation to inhibit LTP induction via a form of negative metaplasticity (Zorumski and Izumi, 2012). In these cases, even brief applications of such stressors can disrupt LTP for a prolonged period following removal of the stressor, and this form of LTP inhibition can be prevented by the NMDAR antagonist D-APV when coapplied with the stressor. Similar to these prior observations, we found that the administration of 1 or 10 μg/ml LPS for 10 min, with LPS washout 30 min before HFS, prevented

LTP induction [100.5 ± 3.4% of baseline with 1 μg/ml LPS ($N = 5$, $p = 0.0005$) vs control LTP; Fig. 3*B*]. Consistent with an NMDAR-mediated metaplastic mechanism, this persisting form of LTP inhibition by LPS was blocked by cotreatment with APV during the period of LPS administration (10 μg/ml LPS, 91.2 ± 6.3%; vs LPS + APV, 133.9 ± 6.8%; $N = 5$ each; $p = 0.0018$; Fig. 3*C*).

To determine whether microglial activation contributes to the effects of LPS, a known proinflammatory stimulus, on LTP, we used minocycline, an anti-inflammatory agent that inhibits microglial-mediated inflammatory activation (Tikka and Koistinaho, 2001; Wu et al., 2015). In the presence of 0.5 μM minocycline, 1 μg/ml LPS failed to block LTP [142.3 ± 10.5% ($N = 5$, $p = 0.0053$) vs LPS alone; Fig. 4*A*]. We also attempted to deplete microglia by feeding mice PLX5622, a colony-stimulating factor 1 receptor antagonist, for 7–14 d postweaning (Henry et al., 2020; Liu et al., 2021). LTP induction remained intact in mice fed a control diet (AIN-76A), and 1 μg/ml LPS inhibited LTP in slices from these mice [control LTP, 161.6 ± 13.0% ($N = 4$) vs LPS-treated slices, 93.6 ± 5.4% ($N = 4$; $p = 0.0029$)]. LTP, however, could not be induced in mice fed PLX5622 [101.6 ± 7.7% ($N = 4$; $p = 0.0075$) vs LTP in control mice].

Prior studies indicate that LPS can act on microglia through cell surface receptor and intracellular mechanisms, including activation of Toll-like receptor 4 (TLR4; Gaikwad and Agrawal-Rajput, 2015). To probe these potential mechanisms, we initially examined the effects of LPS-RS, an LPS derivative that antagonizes both TLR4-dependent and TLR4-independent effects of LPS in microglia and other cells (Kutuzova et al., 2001; Gaikwad and Agrawal-Rajput, 2015). When slices were pretreated with 3 μg/ml LPS-RS for 15 min before and during 15 min LPS exposure, we found that LPS no longer inhibited CA1 LTP acutely [173.1 ± 5.9% ($N = 5$; $p = 0.0015$) vs LPS alone; Fig. 4*B*]. When administered alone, LPS-RS had no significant effect on LTP compared with naive controls [157.6 ± 11.3% ($N = 5$; $p = 0.1479$) vs control LTP; Fig. 4*B*]. Because LPS can activate TLR4, we also examined the effects of two selective TLR4 antagonists, IAXO-102 (Huggins et al., 2015) and TAK-242 (Matsunaga et al., 2011); neither of these TLR4 antagonists altered LTP inhibition by LPS. At a concentration of 5 μM, IAXO-102 did not acutely alter the effects of LPS [109.4 ± 4.6% ($N = 5$, $p = 0.2937$) vs LPS alone; Fig. 4*C*]. Similarly, TAK-242 (1 μM) failed to alter LTP block by LPS [107.3 ± 5.2% ($N = 5$, $p = 0.4844$) vs LPS alone; Fig. 4*D*]. A longer administration of TAK-242 (1 h total) also failed to overcome LPS (97.2 ± 5.8% change; $N = 4$).

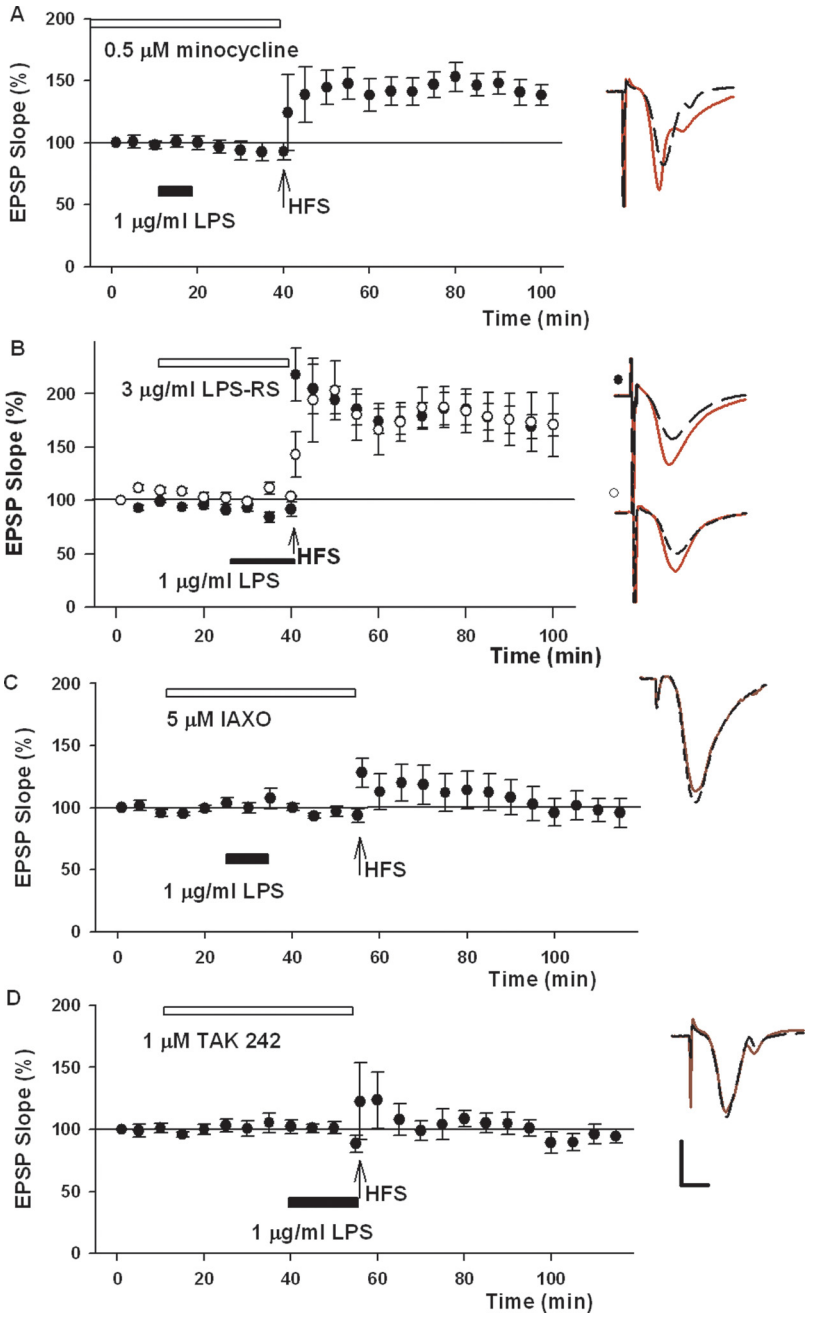

Figure 4. Minocycline and LPS-RS, but not selective TLR4 antagonists, overcome the effects of LPS on LTP. ***A***, At 0.5 μM, the microglial inhibitor, minocycline (white bar) overcomes the persistent effects of LPS (black bar) on LTP. ***B***, At 3 μg/ml, the LPS antagonist LPS-RS prevented the acute effects of 1 μg/ml LPS on LTP (black circles). Administration of LPS-RS alone did not affect LTP (white circles). ***C***, ***D***, In contrast to LPS-RS, two selective TLR4 antagonists (IAXO and Tak 242) failed to alter the ability of 1 μg/ml LPS (black bars) to inhibit LTP. Traces show representative EPSPs. Calibration: 1 mV, 5 ms.

Using hippocampal slices prepared from *Ch25h* KO mice (Bauman et al., 2009), we examined whether the effects of LPS on *Ch25h* and 25HC observed in biochemical studies (Fig. 1) are related to LPS-induced changes in LTP. In slices from both wild-type and *Ch25h* KO mice, LTP was readily induced [wild type: 144.8 ± 7.4% of baseline ($N = 5$; Fig. 5*A*, white circles); KO: 151.8 ± 13.8% change 60 min after HFS ($N = 5$; Fig. 5*A*, white squares; $p = 0.9571$)]. In wild-type mice, LPS readily inhibited LTP induction (97.9 ± 4.9% vs control LTP; $N = 5$; $p = 0.0240$; Fig. 5*B*, black circles). Even in the presence of LPS, HFS induced robust LTP in slices from KO mice [140.4 ± 5.7% ($p = 0.9883$) vs control LTP in wild-type mice; Fig. 5*B*, black squares; overall two-way ANOVA, $p = 0.0088$ for these four groups]. We also

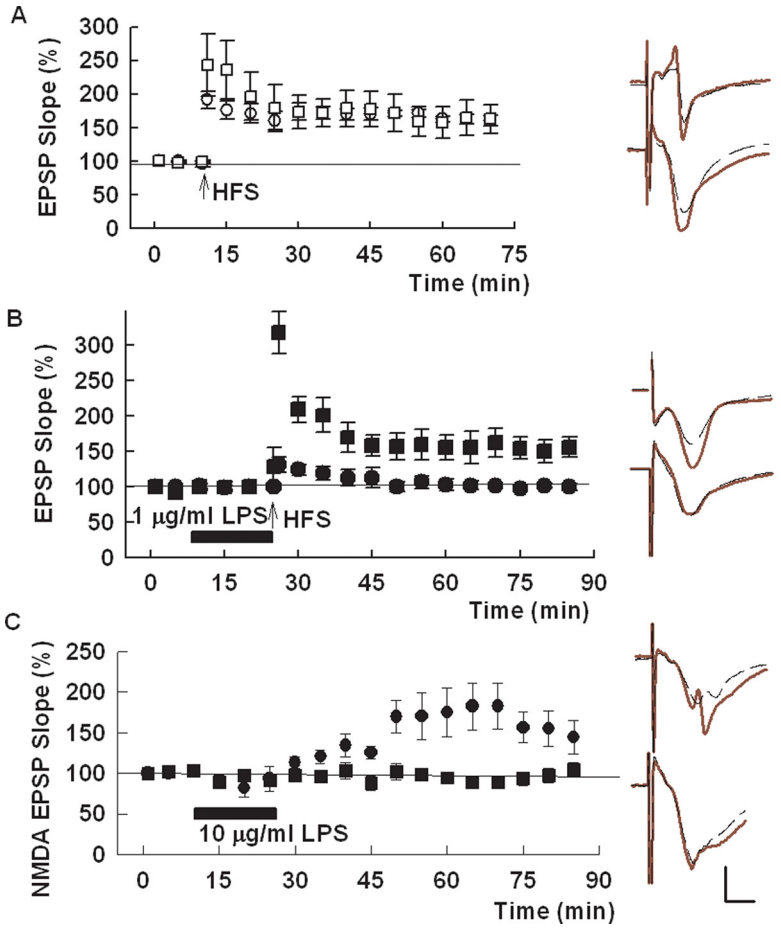

Figure 5. LPS inhibits LTP in slices from wild-type mice but not *Ch25h* KO mice. ***A***, Both wild-type (white circles) and *Ch25h* KO (white squares) slices exhibit robust LTP under baseline conditions. ***B***, LPS (black bar) inhibits LTP in slices from wild-type slices (black circles) but not *Ch25h* KO slices (black squares). ***C***, In slices from wild-type mice, 10 µg/ml LPS × 15 min augmented NMDAR-mediated EPSPs (black circles); in KO slices, LPS had no effect (black squares). Traces to the right of the graphs show representative EPSPs at baseline (dashed traces) and 60 min following HFS or LPS (red traces). Calibration: 1 mV, 5 ms.

found that the ability of 10 µg/ml LPS to augment NMDAR-mediated EPSPs was eliminated in slices from *Ch25h* KO mice [wild type, 128.6 ± 7.7% of baseline ($N = 5$) vs KO, 93.6 ± 3.1% ($N = 6$; $p = 0.0015$; Fig. 5*C*)].

The results outlined above indicate that LPS-mediated LTP inhibition is likely mediated by 25HC. These observations prompted us to examine whether exogenously administered 25HC mimics the effects of LPS on LTP and NMDAR-mediated EPSPs in rat hippocampal slices. Similar to LPS, pretreatment of hippocampal slices with 10 μM 25HC for 15 min just before HFS completely inhibited LTP [97.7 ± 5.7% of baseline 60 min following HFS ($N = 5$, $p = 0.0011$) vs control LTP; Fig. 6*A*]. The effect of 25HC on LTP was not mimicked by its unnatural enantiomer (10 μM), indicating structural selectivity for the inhibition of LTP [154.3 ± 9.3% ($N = 6$, $p = 0.0008$) vs natural 25HC; Fig. 6*A*]. Even at 10 μM, 25HC did not inhibit isolated NMDAR responses but rather produced a small, but variable, enhancement (128.7 ± 16.1%; $N = 9$; Fig. 6*B*; Linsenbardt et al., 2014). Similar to LPS, 1 or 10 μM 25HC administered for 10 min and then washed out 30 min before HFS resulted in a persisting block of LTP [1 μM, 90.9 ± 7.6% ($N = 5$, Fig. 6*C*); 10 μM, 89.0 ± 6.6% ($N = 5$, Fig. 6*D*)]. As with LPS, this prolonged LTP inhibition was completely reversed by coapplication of APV during 25HC exposure [158.3 ± 20.4% ($N = 5$, $p = 0.014$) vs 10 μM 25HC; Fig. 6*D*].

Because our results suggest that 25HC likely acts downstream of microglia activation by LPS, we examined whether minocycline altered the effects of 25HC on LTP. In contrast to LPS, we found that minocycline failed to block the inhibition of LTP by 10 μM 25HC (99.6 ± 6.5%, $N = 5$; Fig. 7*A*). Also in contrast to LPS (Fig. 5), we found that 10 μM 25HC acutely inhibited LTP in slices from *Ch25h*-deficient mice [104.1 ± 5.4% ($N = 7$; $p = 0.0041$) vs control LTP in *Ch25h* KO mice; Fig. 7*B*]. Because 25HC appears to act as a weak partial agonist and functional noncompetitive antagonist at a putative oxysterol site on NMDARs (Paul et al., 2013; Linsenbardt et al., 2014), we also examined whether the effects of 25HC on LTP are altered in hippocampal slices from mice deficient in CYP46A1, the enzyme responsible for synthesis of 24S-HC (Russell et al., 2009), a full agonist positive allosteric modulator of NMDARs (Linsenbardt et al., 2014). In slices from CYP46A1 knock-out mice (Lund et al., 2003) that we previously showed has intact LTP (Sun et al., 2016a), we found that LTP was not induced in the presence of 10 μM 25HC (103.8 ± 7.0%; $N = 4$; Fig. 7*C*).

To determine whether 25HC contributes to *in vivo* effects of LPS, we examined the ability of LPS to alter LTP when administered systemically to wild-type and *Ch25h* KO mice. For these experiments, mice were treated with 1 mg/kg (i.p.) LPS at times ranging from 1 to 24 h before hippocampal slice preparation. In slices from wild-type mice, *in vivo* LPS completely inhibited LTP at all times >1 h after injection (24 h after LPS injection wild-type mice exhibited EPSPs that were 102.4 ± 4.5% of baseline 60 min following HFS, $N = 6$; Fig. 8*A*, white circles). In contrast, LPS treatment had no effect on LTP in slices from *Ch25h* KO mice [141.0 ± 11.9% of baseline ($N = 6$, $p = 0.0126$) vs LPS in wild-type mice; Fig. 8*A*, white squares].

We also examined whether the effects of LPS on LTP are associated with impaired learning in wild-type and *Ch25h* KO mice. For these experiments, we examined learning acquisition and retention in mice treated with LPS 1 h before testing in a one-trial inhibitory avoidance learning task. In this task, mice are initially placed in the lit compartment of a testing chamber that has illuminated and dark chambers. During the training phase, once mice enter the dark compartment, they are given a footshock and removed from the apparatus. When tested 24 h later, mice are again placed in the lit compartment and allowed to explore the device for up to 300 s, receiving no further shocks. Wild-type mice readily learn this task and remain in the lit compartment for 279.2 ± 20.8 s ($N = 6$) before being removed to their home cage (Fig. 8*B*). Wild-type mice treated with LPS 1 h before initial exposure to the footshock show impaired learning 24 h later (remaining in the lit compartment for 132.0 ± 42.9 s; $N = 9$; Fig. 8*B*). Control *Ch25h* KO mice are indistinguishable from wild-type mice under baseline conditions and spent 290.3 ± 6.3 s ($N = 6$) in the lit compartment on testing 24 h after footshock

(Fig. 8*B*). In contrast to wild-type mice, *Ch25h* KO mice treated with LPS also readily learn the task and remained in the lit compartment for 269.3 ± 28.3 s 24 h after exposure to the footshock ($N = 6$, Fig. 8*B*; $p = 0.0075$ by two-way ANOVA). There is a significant difference between saline-treated control wild-type mice and LPS-treated wild-type mice ($p = 0.0213$; Fig. 8*B*). No difference was observed between LPS-treated KO mice versus saline-treated KO mice ($p = 0.8312$), but there is a significant difference between LPS-treated wild-type mice versus LPS-treated KO mice ($p = 0.0455$).

Notably, both wild-type and KO mice exhibit altered behavior with hypoactivity and weight loss 24 h after LPS [wild-type mice, −3.56 ± 0.23 g ($N = 9$); KO mice, −2.15 ± 0.40 g ($N = 6$); Fig. 8*C*], most likely because of the systemic effects of LPS. In contrast, both wild-type and KO control mice not exposed to LPS show some weight gain 24 h after testing [wild-type mice, 0.68 ± 0.21 g ($N = 6$); KO mice, 0.80 ± 0.18 g ($N = 6$; $p < 0.00001$ by two-way ANOVA); Fig. 8*C*]. There is a significant difference between saline-treated control wild-type mice and LPS-treated wild-type mice in weight change ($p < 0.0001$; Fig. 8*C*). Similarly, there is a significant difference between saline-treated KO mice and LPS-treated KO mice ($p < 0.0001$). There is also a significant difference between LPS-treated wild-type mice and LPS-treated KO mice ($p = 0.0201$). Because of the differences in activity and weight observed 24 h after treatment with LPS, we tested learning at shorter intervals following LPS treatment, as described above, to minimize potential confounds from sickness-related behaviors.

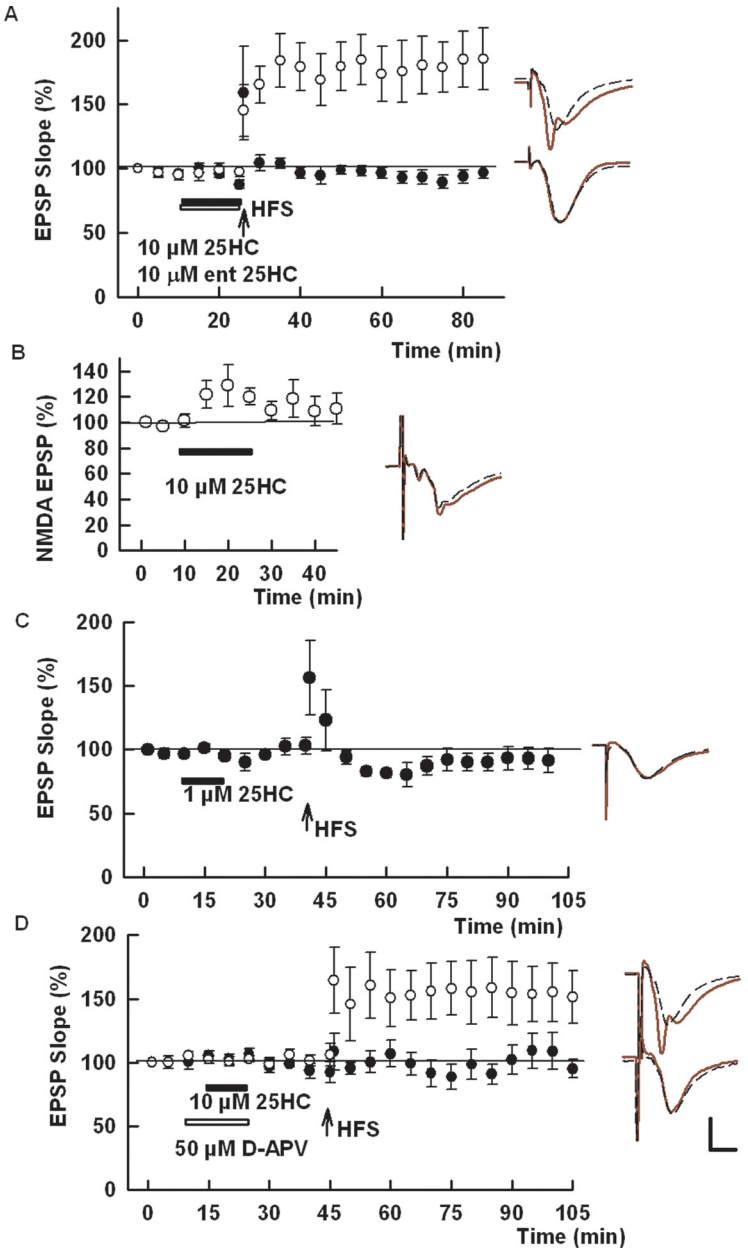

Figure 6. Exogenous 25HC mimics effects of LPS on LTP. ***A***, Administration of 10 μM 25HC for 15 min (black bar) before HFS (arrow) results in LTP inhibition (black circles). At an equimolar concentration, the unnatural enantiomer of 25HC did not alter LTP induction (white bar and circles). ***B***, 25HC does not inhibit NMDAR-mediated EPSPs and results in a small but variable enhancement of these responses. ***C***, Akin to LPS, the administration of 25HC (1 μM) for 10 min (black bar) followed by a 30 min washout before HFS (arrow) also results in LTP inhibition. ***D***, Similar persistent LTP inhibition was observed with 10 μM 25HC (black bar, black circles), and this LTP block was overcome by treatment with the NMDAR antagonist, D-APV (white bar, white circles). Traces to the right of the graph show representative EPSPs, as in other figures. Calibration: 1 mV, 5 ms.

Discussion

The present results demonstrate that microglial activation by LPS, a known proinflammatory stimulus, markedly increases the expression of *Ch25h* and the synthesis of 25HC, and that LPS and 25HC disrupt hippocampal LTP via NMDAR-mediated metaplasticity. Thus, LPS-induced microglial activation adds to neuronal and synaptic stressors that impair LTP via metaplastic mechanisms (Zorumski and Izumi, 2012). Other stressors include metabolic challenges (low glucose) and agents associated with neural toxicity, including ethanol and corticosterone (Zorumski and Izumi, 2012; Zorumski et al., 2014). In all of these examples, the administration of the NMDAR antagonist APV during the stress prevents persisting adverse effects on LTP. Whether microglial activation and 25HC contribute to the effects of other stressors remains to be determined, although these various stressors are known to disrupt learning and memory (Zorumski and Izumi, 2012).

Prior studies have shown that LPS can disrupt LTP when administered *in vivo* or in *ex vivo* slices (Nolan et al., 2004; Maggio et al., 2013; Bie et al., 2014). In some cases, LPS increases neuronal excitability (Pascual et al., 2012; Gao et al., 2014) and synthesis of glucocorticoids (Maggio et al., 2013). We previously reported that corticosterone promotes NMDAR-dependent LTP inhibition (Izumi et al., 2015). LPS also promotes aerobic glycolysis in microglia via TLR4, resulting in the release of interleukin-1β (IL-1β) and LTP inhibition (York et al., 2021). Additionally, LPS promotes hippocampal long-term depression (LTD) when

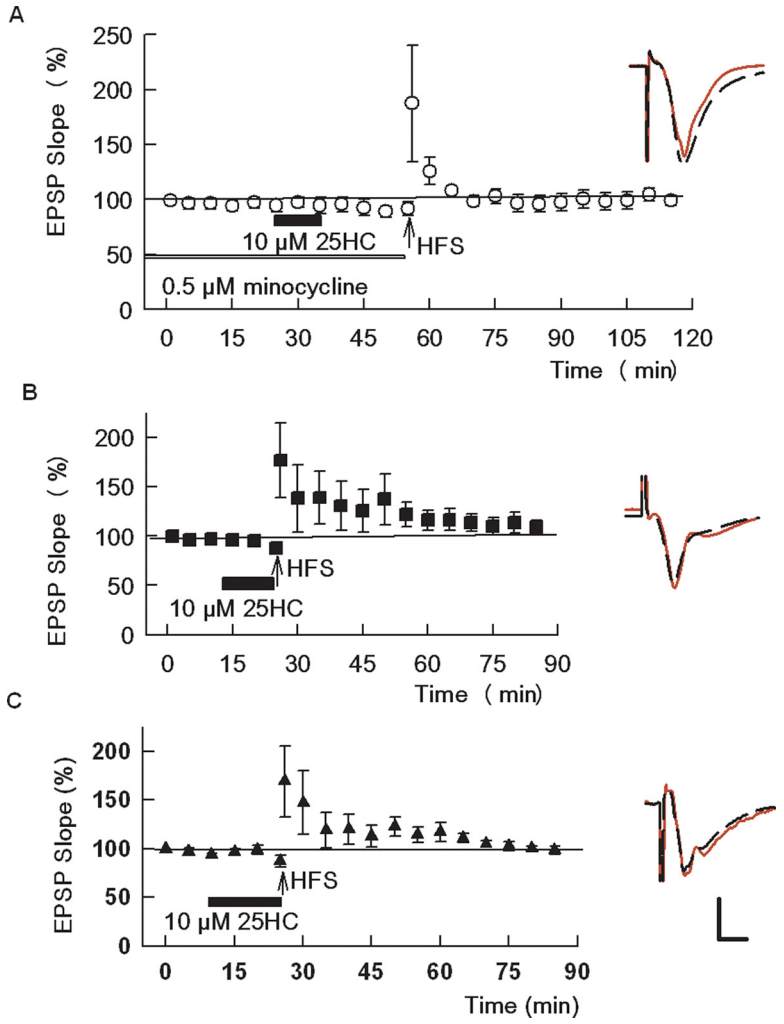

Figure 7. Minocycline does not alter the effects of 25HC on LTP and 25HC inhibits LTP in slices from *Ch25h* and CYP46A1 KO mice. ***A***, Unlike LPS, minocycline (white bar) failed to alter persistent LTP inhibition by 25HC (black bar). ***B***, ***C***, 25HC inhibited LTP in slices from *Ch25h* KO mice (***B***) and CYP46A1 KO mice (***C***). Traces to the right of the graphs show representative EPSPSs, as in prior figures. Calibration: 1 mV, 5 ms.

administered in combination with a metabolic stressor through a mechanism that involves complement receptor 3 (CR3), but not TLR4 (Zhang et al., 2014a). Similarly, we found that the induction of LTD by low-frequency synaptic stimulation produces metaplastic LTP inhibition (Izumi et al., 2013). The ability of LPS to enhance hippocampal excitability (Pascual et al., 2012; Gao et al., 2014) is consistent with effects on LTP via NMDAR activation, shown here. However, LPS produced no change in AMPAR EPSPs when administered before LTP induction, suggesting that the increase in NMDAR EPSPs is likely postsynaptic in origin. LPS may also disrupt LTP via MAPK activation (Nolan et al., 2004), and we have found that p38 MAPK contributes to metaplastic LTP inhibition (Izumi et al., 2008). Whether LPS activates other modulators involved in metaplastic LTP inhibition, including nitric oxide (Izumi et al., 1992) and the neurosteroid allopregnanolone (Tokuda et al., 2011), requires further study.

Our results indicate that microglial activation by LPS promotes synthesis of the endogenous oxysterol 25HC and that genetic deletion of *Ch25h* abrogates LPS-induced LTP inhibition. Our biochemical studies were based on 24 h incubations in a low concentration of LPS (e.g., 10 ng/ml). We also found that 10–100 ng/ml LPS inhibited LTP when administered for 2–3 h (Fig. 2), and the effects on LTP were mimicked by shorter duration exposures to higher concentrations. Additionally, wild-type microglia have higher baseline levels of 25HC compared with *Ch25h* KO microglia, and these differences may contribute to effects seen with shorter applications of LPS. Our experiments do not distinguish whether short exposures to LPS promote the release of basal 25HC or newly synthesized oxysterol, but we note that prior studies observed changes in hippocampal excitability with shorter duration exposures (5–30 min), including rapid production and release of neuromodulators (Pascual et al., 2012; Gao et al., 2014; Tzour et al., 2017).

In our study, microglial activation by LPS appears independent of TLR4, a pattern recognition receptor activated by LPS, although LPS also stimulates CR3 (Zhang et al., 2014a) and can have direct intracellular effects via noncanonical inflammasome activation (Shi et al., 2014). Inhibition of the effects of LPS on LTP by LPS-RS, but not more selective TLR4 inhibitors, is consistent with the known direct effects of LPS-RS on LPS internalization and caspase-11 (Kutuzova et al., 2001; Shi et al., 2014). However, LPS-RS also inhibits TLR4 (Coats et al., 2005; Gaikwad and Agrawal-Rajput, 2015), making it likely that multiple mechanisms contribute to the effects we observed. We also note that certain effects of LPS on hippocampal plasticity in other studies were independent of TLR4 (Zhang et al., 2014a). Our results differ from observations in cultured mouse bone marrow-derived macrophages where LPS markedly stimulates *Ch25h* expression in wild-type cells but not TLR4-deficient cells (Diczfalusy et al., 2009). Differences in cell types and tissue preparation may account for differences we observed using selective TLR4 antagonists, although significant increases in *Ch25h* expression were observed in macrophages by 2 h (the shortest time studied), consistent with the time course of LTP inhibition that we observed with LPS (in nanograms per milliliter) in hippocampal slices.

Effects of LPS on LTP are mimicked by exogenously administered 25HC in both wild-type and *Ch25h*-deficient mice, indicating structural sterol selectivity. These results are consistent with studies in peripheral inflammatory cells where 25HC is the major endogenous oxysterol synthesized and released from macrophages (Blanc et al., 2013). The Brain RNA-Seq database suggests that mouse *Ch25h* as well as human *CH25H* are expressed largely, if not exclusively, in microglia (Zhang et al., 2014b). In the periphery, 25HC has complex effects on inflammatory responses and has been described as a "context-dependent" modulator (Fessler, 2016) with both positive and negative effects on inflammatory responses (Gold et al., 2014; Reboldi et al., 2014; Jang et al., 2016; Mutemberezi et al., 2018). Recent studies

in microglia indicate that LPS promotes the production of proinflammatory cytokines IL-1β and IL-1α, and these effects are dampened in *Ch25h*-KO animals (Wong et al., 2020). In contrast, LPS-stimulated production of TNFα and IL-6 is not altered in these knock-out mice (Wong et al., 2020). The ability of 25HC to promote LPS-stimulated IL-1β induction in microglia is also enantioselective, consistent with what we observed in our LTP experiments (Wong et al., 2020).

25HC has several actions that could contribute to LTP inhibition. We previously found that 25HC is a partial agonist at a putative oxysterol site on NMDARs, with weak ability to enhance NMDAR responses while dampening the effect of more effective agonists such as 24S-HC (Linsenbardt et al., 2014). Effects against oxysterol NMDAR PAMs is noncompetitive and enantioselective (Linsenbardt et al., 2014). Here we found that effects of 25HC against LTP are not mimicked by ent-25HC at an equimolar concentration. Inhibitory effects of 25HC on 24S-HC appear unlikely to contribute to effects on LTP because 25HC dampens LTP in slices from CYP46A1-deficient mice that do not produce significant amounts of 24S-HC (Sun et al., 2016a), and we previously found that 24S-HC promotes rather than inhibits LTP (Paul et al., 2013; Izumi et al., 2021). In contrast, 25HC regulates cellular cholesterol homeostasis, although these effects are nonenantioselective in contrast to what we have observed with LTP (Olsen et al., 2012). 25HC also activates the integrated stress response (ISR) via GCN2 kinase (Shibata et al., 2013). Activation of ISR as a mechanism to inhibit LTP is consistent with the ability of ISRIB, a small-molecule ISR inhibitor, to promote synaptic plasticity and learning in other studies (Sidrauski et al., 2013; Di Prisco et al., 2014; Chou et al., 2017), including the ability to overcome metaplastic LTP inhibition by NMDA and ethanol (Izumi and Zorumski, 2020). Activation of endoplasmic reticulum (ER) cellular stress responses also promotes the movement of cholesterol from ER to mitochondria, resulting in the production of pregnenolone (Barbero-Camps et al., 2014), the first step in the synthesis of neurosteroids such as allopregnanolone, a modulator involved in metaplastic LTP inhibition (Tokuda et al., 2011). 25HC also has complex effects on inflammasomes and can promote the release of inflammatory cytokines such as interleukin-1β that can have adverse effects on synaptic function (Gold et al., 2014; Jang et al., 2016; Wong et al., 2020). While we did not examine intracellular mechanisms contributing to the effects of LPS or 25HC, we have previously found that NMDAR-mediated LTP inhibition, akin to what we observed here, involves complex signaling including phosphatases, nitric oxide synthase, and p38 MAPK (Zorumski and Izumi, 2012). It will be important to pursue these cellular mechanisms in future studies, including the effects of LPS and 25HC on both NMDAR function and LTP. Nonetheless, 25HC appears to be a key mediator of the effects of LPS based on observations in Ch25h-deficient slices, likely in part via direct effects on NMDARs (Linsenbardt et al., 2014).

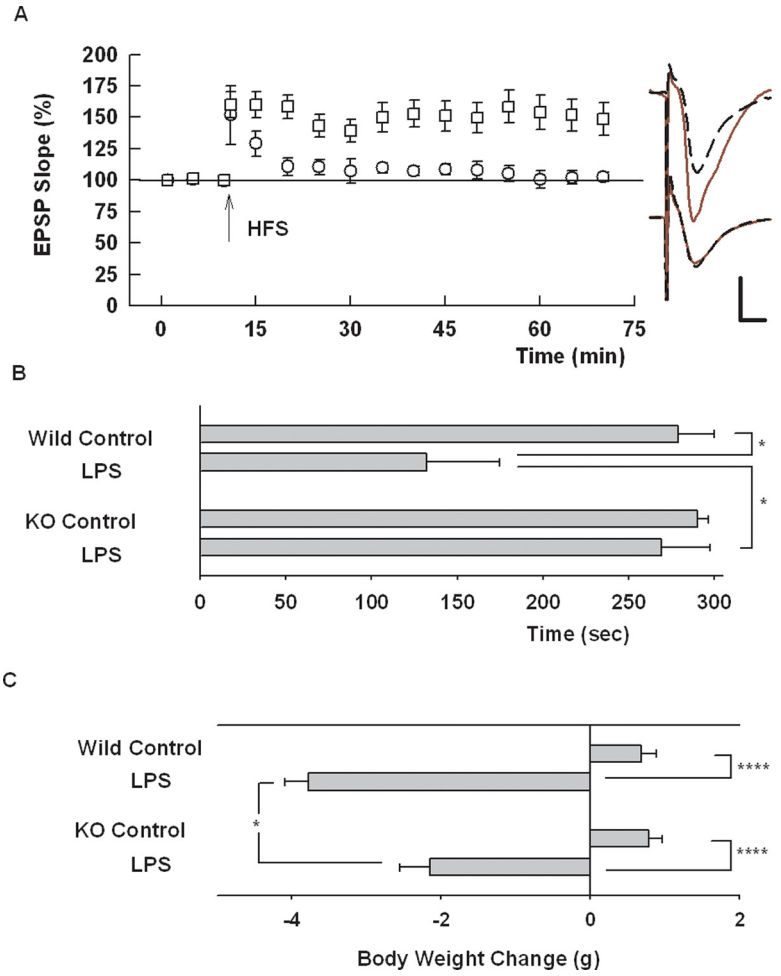

Figure 8. Effects of LPS *in vivo*. ***A***, Administration of LPS (1 mg/kg, i.p.) $\geq$1 h before hippocampal slice preparation results in a defect in LTP induction in wild-type mice (white circles). In contrast, similar administration of LPS in *Ch25h* KO mice does not alter LTP (white squares). Traces to the right of the graph show representative EPSPs. Calibration: 1 mV, 5 ms. ***B***, In wild-type mice, LPS administered 1 h before inhibitory avoidance training results in a defect in learning as manifested by mice more readily leaving the lit chamber to enter the dark chamber where they had received a footshock 24 h previously. In contrast, LPS had no effect on learning in *Ch25h* KO mice. ***C***, LPS resulted in weight loss 24 h following administration in both wild-type and KO mice, although the amount of weight loss was less in the KO mice. *$p < 0.05$; ****$p < 0.0001$ by two-way ANOVA.

Neuropsychiatric illnesses are major causes of death and disability, and major depression is a leading cause of disability worldwide. Importantly, neuroinflammatory changes in brain are thought to contribute significantly to the pathophysiology of these illnesses and represent potentially novel targets for therapeutic interventions (Kiecolt-Glaser et al., 2015; Yirmiya et al., 2015). While neuroinflammation contributes to multiple facets of neuropsychiatric disorders including illness-related behaviors (pain, sleep, and appetite changes), the effects of inflammation on synaptic function may be a major contributor to illness-related disability. The results presented here indicate that 25HC is an important endogenous modulator that can be released from microglia to mediate the effects of an inflammatory stimulus on hippocampal network function and learning. Hence, these studies provide a potential avenue for novel treatments for cognitive dysfunction in a range of disorders, and thus represent potential strategies to reduce societal impact and devastating consequences of certain neuropsychiatric illnesses, including perhaps longer-term sequelae of COVID-19 (Wang et al., 2020).

References

Barbero-Camps E, Fernández A, Baulies A, Martinez L, Fernández-Checa JC, Colell A (2014) Endoplasmic reticulum stress mediates amyloid β neurotoxicity via mitochondrial cholesterol trafficking. Am J Pathol 184:2066–2081.

Bauman DR, Bitmansour AD, McDonald JG, Thompson BM, Liang G, Russell DW (2009) 25-Hydroxycholesterol secreted by macrophages in response to Toll-like receptor activation suppresses immunoglobulin A production. Proc Natl Acad Sci U S A 106:16764–16769.

Bie B, Wu J, Yang H, Xu JJ, Brown DL, Naguib M (2014) Epigenetic suppression of neuroligin 1 underlies amyloid-induced memory deficiency. Nat Neurosci 17:223–231.

Blanc M, Hsieh WY, Robertson KA, Kropp KA, Forster T, Shui G, Lacaze P, Watterson S, Griffiths SJ, Spann NJ, Meljon A, Talbot S, Krishnan K, Covey DF, Wenk MR, Craigon M, Ruzsics Z, Haas J, Angulo A, Griffiths WJ, et al. (2013) The transcription factor STAT-1 couples macrophage synthesis of 25-hydroxycholesterol to the interferon antiviral response. Immunity 38:106–118.

Bohlen CJ, Bennett FC, Tucker AF, Collins HY, Mulinyawe SB, Barres BA (2017) Diverse requirements for microglial survival, specification, and function revealed by defined-medium cultures. Neuron 94:759–773.

Chou A, Krukowski K, Jopson T, Zhu PJ, Costa-Mattioli M, Walter P, Rosi S (2017) Inhibition of the integrated stress response reverses cognitive deficits after traumatic brain injury. Proc Natl Acad Sci U S A 114:E6420–E6426.

Coats SR, Pham T-TT, Bainbridge W, Reife RA, Darveau RP (2005) MD-2 mediates the ability of tetra-acylated and penta-acylated lipopolysaccharides to antagonize *Escherichia coli* lipopolysaccharide at the TLR4 signaling complex. J Immunol 175:4490–4498.

Diczfalusy U, Olofsson KE, Carlsson A-M, Gong M, Golenbock DT, Rooyackers O, Fläring U, Björkbacka H (2009) Marked upregulation of cholesterol 25-hydroxylase expression by lipopolysaccharide. J Lipid Res 50:2258–2264.

Di Prisco GV, Huang W, Buffington SA, Hsu C-C, Bonnen PE, Placzek AN, Sidrauski C, Krnjević K, Kaufman RJ, Walter P, Costa-Mattioli M (2014) Translational control of mGluR-dependent long-term depression and object-place learning by eIF2α. Nat Neurosci 17:1073–101082.

Fessler MB (2016) The intracellular cholesterol landscape: dynamic integrator of the immune response. Trends Immunol 37:819–830.

Gaikwad S, Agrawal-Rajput R (2015) Lipopolysaccharide from *Rhodobacter sphaeroides* attenuates microglia-mediated inflammation and phagocytosis and directs regulatory T cell response. Int J Inflamm 2015:361326.

Gao F, Liu Z, Ren W, Jiang W (2014) Acute lipopolysaccharide exposure facilitates epileptiform activity via enhanced excitatory synaptic transmission and neuronal excitability in vitro. Neuropsychiatr Dis Treat 10:1489–1495.

Gold ES, Diercks AH, Podolsky I, Podyminogin RL, Askovich PS, Treuting PM, Aderem A (2014) 25-Hydroxycholesterol acts as an amplifier of inflammatory signaling. Proc Natl Acad Sci U S A 111:10666–10671.

Henry RJ, Ritzel RM, Barrett JP, Doran SJ, Jiao Y, Leach JB, Szeto GL, Wu J, Stoica BA, Faden AI, Loane DJ (2020) Microglial depletion with CSF1R inhibitor during chronic phase of experimental traumatic brain injury reduces neurodegeneration and neurological deficits. J Neurosci 40:2960–2974.

Hodes GE, Kana V, Menard C, Merad M, Russo SJ (2015) Neuroimmune mechanisms of depression. Nat Neurosci 18:1386–1393.

Huggins C, Pearce S, Peri F, Neumann F, Cockerill G, Pirianov G (2015) A novel small molecule TLR4 antagonist (IAXO-102) negatively regulates non-hematopoietic toll like receptor 4 signalling and inhibits aortic aneurysms development. Atherosclerosis 242:563–570.

Iwata M, Ota KT, Li X-Y, Sakaue F, Li N, Dutheil S, Banasr M, Duric V, Yamanashi T, Kaneko K, Rasmussen K, Glasebrook A, Koester A, Song D, Jones KA, Zorn S, Smagin G, Duman RS (2016) Psychological stress activates the inflammasome via release of adenosine triphosphate and stimulation of the purinergic type 2X7 receptor. Biol Psychiatry 80:12–22.

Izumi Y, Zorumski CF (2020) Inhibitors of cellular stress overcome acute effects of ethanol on hippocampal plasticity and learning. Neurobiol Dis 141:104875.

Izumi Y, Clifford DB, Zorumski CF (1992) Inhibition of long-term potentiation by NMDA-mediated nitric oxide release. Science 257:1273–1276.

Izumi Y, Nagashima K, Murayama K, Zorumski CF (2005) Acute effects of ethanol on hippocampal long-term potentiation and long-term depression are mediated by different mechanisms. Neuroscience 136:509–517.

Izumi Y, Tokuda K, Zorumski CF (2008) Long-term potentiation inhibition by low-level *N*-methyl-D-aspartate receptor activation involves calcineurin, nitric oxide and p38 mitogen-activated protein kinase. Hippocampus 18:258–265.

Izumi Y, O'Dell KA, Zorumski CF (2013) Metaplastic LTP inhibition after LTD induction in CA1 hippocampal slices involves NMDA receptor-mediated neurosteroidogenesis. Physiol Rep 1:e00133.

Izumi Y, O'Dell KA, Zorumski CF (2015) Corticosterone enhances the potency of ethanol against hippocampal long-term potentiation via local neurosteroid synthesis. Front Cell Neurosci 9:254.

Izumi Y, Mennerick SJ, Doherty JJ, Zorumski CF (2021) Oxysterols modulate the acute effects of ethanol on hippocampal *N*-Methyl-D-aspartate receptors, long-term potentiation, and learning. J Pharmacol Exp Ther 377:181–188.

Jang J, Park S, Hur HJ, Cho H-J, Hwang I, Kang YP, Im I, Lee H, Lee E, Yang W, Kang H-C, Kwon SW, Yu J-W, Kim D-W (2016) 25-Hydroxycholesterol contributes to cerebral inflammation of X-linked adrenoleukodystrophy through activation of the NLRP3 inflammasome. Nat Commun 7:13129.

Jiang X, Ory DS, Han X (2007) Characterization of oxysterols by electrospray ionization tandem mass spectrometry after one-step derivatization with dimethylglycine. Rapid Commun Mass Spectrom 21:141–152.

Kiecolt-Glaser JK, Derry HM, Fagundes CP (2015) Inflammation: depression fans the flames and feasts on the heat. Am J Psychiatry 172:1075–1091.

Kutuzova GD, Albrecht RM, Erickson CM, Qureshi N (2001) Diphosphoryl lipid A from *Rhodobacter sphaeroides* blocks the binding and internalization of lipopolysaccharide in RAW 264.7 cells. J Immunol 167:482–489.

Lathe R, Sapronova A, Kotelevtsev Y (2014) Atherosclerosis and Alzheimer—diseases with a common cause? Inflammation, oxysterols, vasculature. BMC Geriatr 14:36.

Linsenbardt AJ, Taylor A, Emnett CM, Doherty JJ, Krishnan K, Covey DF, Paul SM, Zorumski CF, Mennerick S (2014) Different oxysterols have opposing actions at *N*-methyl-D-aspartate receptors. Neuropharmacol 85:232–242.

Liu Y-J, Spangenberg EE, Tang B, Holmes TC, Green KN, Xu X (2021) Microglia elimination increases neural circuit connectivity and activity in adult mouse cortex. J Neurosci 41:1274–1287.

Lund EG, Kerr TA, Sakai J, Li W-P, Russell DW (1998) cDNA cloning of mouse and human cholesterol 25-hydroxylases, polytopic membrane proteins that synthesize a potent oxysterol regulator of lipid metabolism. J Biol Chem 273:34316–34327.

Lund EG, Xie C, Kotti T, Turley SD, Dietschy JM, Russell DW (2003) Knockout of the cholesterol 24-hydroxylase gene in mice reveals a brain-specific mechanism of cholesterol turnover. J Biol Chem 278:22980–22988.

Luu W, Sharpe LJ, Capell-Hattam I, Gelissen IC, Brown AJ (2016) Oxysterols: old tale, new twists. Annu Rev Pharmacol Toxicol 56:447–467.

Maggio N, Shavit-Stein E, Dori A, Blatt I, Chapman J (2013) Prolonged systemic inflammation persistently modifies synaptic plasticity in the hippocampus: modulation by the stress hormones. Front Mol Neurosci 6:46.

Matsunaga N, Tsuchimori N, Matsumoto T, Ii M (2011) TAK-242 (Resatorvid), a small-molecule inhibitor of toll-like receptor (TLR) 4 signaling, binds selectively to TLR4 and interferes with interactions between TLR4 and its adaptor molecules. Mol Pharmacol 79:34–41.

Min SS, Quan HY, Ma J, Han J-S, Jeon BH, Seol GH (2009) Chronic brain inflammation impairs two forms of long-term potentiation in the rat hippocampal CA1 area. Neurosci Lett 456:20–24.

Mutemberezi V, Buisseret B, Masquelier J, Guillemot-Legris O, Alhouayek M, Muccioli GG (2018) Oxysterol levels and metabolism in the course of neuroinflammation: insights from in vitro and in vivo models. J Neuroinflammation 15:74.

Nolan Y, Martin D, Campbell VA, Lynch MA (2004) Evidence of a protective effect of phosphatidylserine-containing liposomes on lipopolysaccharide-induced impairment of long-term potentiation in the rat hippocampus. J Neuroimmunol 151:12–23.

Olsen BN, Schlesinger PH, Ory DS, Baker NA (2012) Side-chain oxysterols: from cells to membranes to molecules. Biochim Biophys Acta 1818:330–336.

Pascual O, Achour SB, Rostaing P, Triller A, Bessis A (2012) Microglia activation triggers astrocyte-mediated modulation of excitatory neurotransmission. Proc Natl Acad Sci U S A 109:E197–E205.

Paul SM, Doherty JJ, Robichaud AJ, Belfort GM, Chow BY, Hammond RS, Crawford DC, Linsenbardt AJ, Shu H-J, Izumi Y, Mennerick SJ, Zorumski CF (2013) The major brain cholesterol metabolite 24(S)-hydroxycholesterol is a potent allosteric modulator of *N*-methyl-D-aspartate receptors. J Neurosci 33:17290–17300.

Reboldi A, Dang EV, McDonald JG, Liang G, Russell DW, Cyster JG (2014) 25-hydroxycholesterol suppresses interleukin-1-driven inflammation downstream of type I interferon. Science 345:679–684.

Russell DW, Halford RW, Ramirez DMO, Shah R, Kotti T (2009) Cholesterol 24-hydroxylase: an enzyme of cholesterol turnover in the brain. Annu Rev Biochem 78:1017–1040.

Shi J, Zhao Y, Wang Y, Gao W, Ding J, Li P, Hu L, Shao F (2014) Inflammatory caspases are innate immune receptors for intracellular LPS. Nature 514:187–192.

Shibata N, Carlin AF, Spann NJ, Saijo K, Morello CS, McDonald JG, Romanoski CE, Maurya MR, Kaikkonen MU, Lam MT, Crotti A, Reichart D, Fox JN, Quehenberger O, Raetz CRH, Sullards MC, Murphy RC, Merrill AH, Brown HA, Dennis EA, et al. (2013) 25-Hydroxycholesterol activates the integrated stress response to reprogram transcription and translation in macrophages. J Biol Chem 288:35812–35823.

Sidrauski C, Acosta-Alvear D, Khoutorsky A, Vedantham P, Hearn BR, Li H, Gamache K, Gallagher CM, Ang KK-H, Wilson C, Okreglak V, Ashkenazi A, Hann B, Nader K, Arkin MR, Renslo AR, Sonenberg N, Walter P (2013) Pharmacological brake-release of mRNA translation enhances cognitive memory. Elife 2:e00498.

Simon A (2014) Cholesterol metabolism and immunity. N Engl J Med 371:1933–1935.

Sun M-Y, Izumi Y, Benz A, Zorumski CF, Mennerick SJ (2016a) Endogenous 24S-hydroxycholesterol modulates NMDAR-mediated function in hippocampal slices. J Neurophysiol 115:1263–1272.

Sun M-Y, Linsenbardt A, Emnett C, Eisenman LN, Izumi Y, Zorumski C, Mennerick S (2016b) 24(S)-Hydroxycholesterol as a modulator of neuronal signaling and survival. Neuroscientist 22:132–144.

Tikka TM, Koistinaho JE (2001) Minocycline provides neuroprotection against N-methyl-D-aspartate neurotoxicity by inhibiting microglia. J Immunol 166:7527–7533.

Tokuda K, O'Dell KA, Izumi Y, Zorumski CF (2010) Midazolam inhibits hippocampal long-term potentiation and learning through dual central and peripheral benzodiazepine receptor activation and neurosteroidogenesis. J Neurosci 30:16788–16795.

Tokuda K, Izumi Y, Zorumski CF (2011) Ethanol enhances neurosteroidogenesis in hippocampal pyramidal neurons by paradoxical NMDA receptor activation. J Neurosci 31:9905–9909.

Tzour A, Leibovich H, Barkai O, Biala Y, Lev S, Yaari Y, Binshtok AM (2017) K_V7/M channels as targets for lipopolysaccharide-induced inflammatory neuronal hyperexcitability. J Physiol 595:713–738.

Waltl S, Patankar JV, Fauler G, Nusshold C, Ullen A, Eibinger G, Wintersperger A, Kratky D, Malle E, Sattler W (2013) 25-Hydroxycholesterol regulates cholesterol homeostasis in the murine CATH.a neuronal cell line. Neurosci Lett 539:16–21.

Wang S, Colonna M (2019) Microglia in Alzheimer's disease: a target for immunotherapy. J Leukoc Biol

Wang S, Li W, Hui H, Tiwari SK, Zhang Q, Croker BA, Rawlings S, Smith D, Carlin AF, Rana TM (2020) Cholesterol 25-hydroxylase inhibits SARS-CoV-2 and other coronaviruses by depleting membrane cholesterol. EMBO J 39:e106057.

Westover EJ, Covey DF (2006) Synthesis of ent-25-hydroxycholesterol. Steroids 71:484–488.

Whitlock JR, Heynen AJ, Shuler MG, Bear MF (2006) Learning induces long-term potentiation in the hippocampus. Science 313:1093–1097.

Wohleb ES, Franklin T, Iwata M, Duman RS (2016) Integrating neuroimmune systems in the neurobiology of depression. Nat Rev Neurosci 17:497–511.

Wong MY, Lewis M, Doherty JJ, Shi Y, Cashikar AG, Amelianchik A, Tymchuk S, Sullivan PM, Qian M, Covey DF, Petsko GA, Holtzman DM, Paul SM, Luo W (2020) 25-Hydroxycholesterol amplifies microglial IL-1β production in an apoE isoform-dependent manner. J Neuroinflammation 17:192.

Wu Y, Dissing-Olesen L, MacVicar BA, Stevens B (2015) Microglia: dynamic mediators of synapse development and plasticity. Trends Immunol 36:605–613.

Yirmiya R, Rimmerman N, Reshef R (2015) Depression as a microglial disease. Trends Neurosci 38:637–658.

York EM, Zhang J, Choi HB, MacVicar BA (2021) Neuroinflammatory inhibition of long-term potentiation requires immunometabolic reprogramming of microglia. Glia 69:567–578.

Zhang HJ, Malik A, Choi HB, Ko RWY, Dissing-Olesen L, MacVicar BA (2014a) Microglial CR3 activation triggers long-term synaptic depression in the hippocampus via NADPH oxidase. Neuron 82:195–207.

Zhang Y, Chen K, Sloan SA, Bennett ML, Scholze AR, O'Keeffe S, Phatnani HP, Guarnieri P, Caneda C, Ruderisch N, Deng S, Liddelow SA, Zhang C, Daneman R, Maniatis T, Barres BA, Wu JQ (2014b) An RNA-sequencing transcriptome and splicing database of glia, neurons, and vascular cells of the cerebral cortex. J Neurosci 34:11929–11947.

Zorumski CF, Izumi Y (2012) NMDA receptors and metaplasticity: mechanisms and possible roles in neuropsychiatric disorders. Neurosci Biobehav Rev 36:989–1000.

Zorumski CF, Mennerick S, Izumi Y (2014) Acute and chronic effects of ethanol on learning-related synaptic plasticity. Alcohol 48:1–17.